

Regression Equations for Calculation of Z Scores of Cardiac Structures in a Large Cohort of Healthy Infants, Children, and Adolescents: An Echocardiographic Study

Michael D. Pettersen, MD, Wei Du, PhD, Mary Ellen Skeens, MS, and Richard A. Humes, MD, *Detroit Michigan; and Andover, Massachusetts*

Background: Decision making in the care of pediatric patients with congenital and acquired heart disease remains reliant on detailed measurements of cardiac structures using 2-dimensional echocardiography. Calculated z scores are often used to normalize these measurements to the patient's body size. Existing normal data in the literature are limited by small sample size, small numbers of measured cardiac structures, and inadequate data for the calculation of z scores. Accordingly, we sought to develop normative data in a large pediatric cohort using modern echocardiographic equipment from which z scores could be calculated.

Methods: Two-dimensional and M-mode echocardiography was performed in 782 patients ranging in age from 1 day to 18 years. Measurements were made of 21 individual cardiac structures. Regression equations were derived to relate the size of the various cardiac structures to body surface area. Data are presented graphically, and regression equations are derived relating cardiac dimension to body surface area.

Conclusion: The presented data will allow the calculation of z scores for echocardiographically measured cardiac structures. This information will be valuable for clinicians caring for infants and children with known or suspected cardiac disease.

Keywords: Adolescents, Children, Echocardiography, Infants, Reference values

Despite the many technologic advances available for the anatomic and hemodynamic evaluation of cardiac pathology, measurement of cardiac structures by 2-dimensional echocardiography remains a fundamental aspect of diagnosis and medical decision making in children with congenital heart and acquired heart disease. Because of growth throughout childhood, interpretation of these measurements requires normalization of the dimensions of cardiac structures to the size of the body. This is commonly done by the calculation of z scores for the measurement of interest. Currently available normative data in the medical literature are limited by the techniques used to obtain the measurements, small sample sizes, limited age ranges, a small number of measured cardiac structures, or insufficient data for the calculation of z scores.

The purpose of this study is to generate normative data of the 2-dimensional or 2-dimensionally guided M-mode echocardiographic

measurements for each of 21 commonly measured cardiac structures in a large cohort of normal infants, children, and adolescents. A regression equation for each parameter was generated to allow the calculation of z scores. This report represents the largest normative pediatric data set available in the medical literature.

MATERIALS AND METHODS

Study Patients

The study population consisted of 813 patients aged 1 day to 18 years (median age 70 months) who were evaluated in the echocardiography laboratory at the Children's Hospital of Michigan between July 1, 2001, and September 30, 2003. Thirty-one patients had missing data for height or weight, leaving 782 patients available for analysis. Patients included in the study had no clinical, electrocardiographic, chest x-ray, or echocardiographic evidence of congenital or acquired cardiac disease. Most patients were being evaluated for the presence of a cardiac murmur, chest pain, or syncope. The presence of a patent ductus arteriosus in the first 3 days of life or a patent foramen ovale was considered to be normal. Included patients with a patent ductus arteriosus had no greater than a small left-to-right shunt. Patients with congenital or acquired heart disease, known or suspected neuromuscular disease, genetic syndromes or chromosomal abnormalities, obesity, systemic or pulmonary hypertension, recent arrhythmia, connective tissue disease, or family history of genetic cardiac disease (eg, Marfan's syndrome or cardiomyopathy)

From the Carman and Ann Adams Department of Pediatrics, Wayne State University School of Medicine, Detroit, Michigan (M.D.P., W.D., R.A.H.); and Philips Medical Systems, Healthcare Informatics, Andover, Massachusetts (M.E.S.).

Reprint requests: Michael D. Pettersen, MD, Division of Cardiology, Children's Hospital of Michigan, 3901 Beaubien Blvd, Detroit, MI 48201 (E-mail: mpetters@dmc.org).

0894-7317/\$34.00

Copyright 2008 by the American Society of Echocardiography.

doi:10.1016/j.echo.2008.02.006

Table 1 Description of 2-dimensional echocardiographic measurements

Measurement	View	Description
Aortic valve annulus	Parasternal long axis	Distance between hinge points during systole
Sinuses of Valsalva	Parasternal long axis	Maximum systolic dimension
Sinotubular junction	Parasternal long axis	Maximum systolic dimension
Transverse aortic arch	Suprasternal long axis	Maximum systolic dimension between the innominate and left common carotid arteries
Aortic isthmus	Suprasternal long axis	Maximum systolic dimension immediately beyond left subclavian artery
Distal aortic arch	Suprasternal long axis	Maximum systolic dimension immediately beyond aortic isthmus
Aorta at diaphragm	Subcostal long axis	Maximal systolic dimension at the level of the diaphragm
Pulmonary valve annulus	Parasternal long axis	Distance between hinge points during systole
Main pulmonary artery	Parasternal short axis	Maximal systolic dimension
Right pulmonary artery	Suprasternal short axis	Maximal systolic dimension immediately beyond the bifurcation
Left pulmonary artery	Parasternal short axis	Maximal systolic dimension immediately beyond the bifurcation
Mitral valve annulus	Apical 4 chamber	Distance between the hinge points during diastole
Tricuspid valve annulus	Apical 4 chamber	Distance between the hinge points during diastole
Left atrium	Parasternal long axis	Maximum antero-posterior dimension during systole

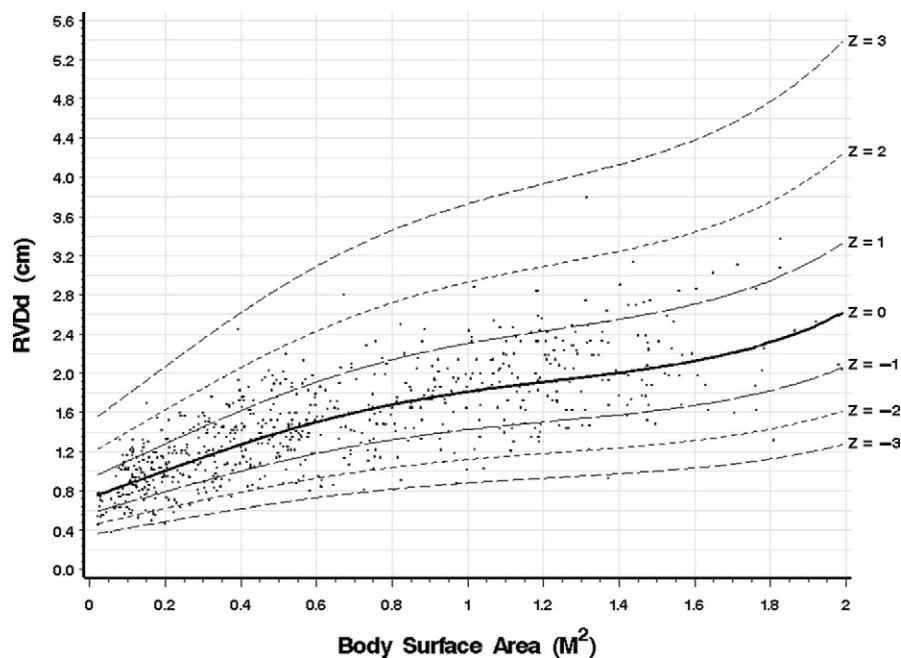


Figure 1 Scatter plots of each of the 21 measured structures plotted against BSA. The superimposed *solid lines* represent the estimated regression equation (labeled as $z = 0$). The superimposed *dashed lines* represent the $\pm 1, 2,$ and $3 z$ values above and below the regression line.

were excluded. Only patients with a technically adequate 2-dimensional evaluation were included. Approval for this study was obtained from the Wayne State University Human Investigations Committee.

Echocardiographic Examination

All patients underwent a complete 2-dimensional, color flow Doppler, and spectral Doppler examination. If necessary, younger patients were sedated to facilitate the examination (intranasal midazolam, 0.2 mg/kg, maximum dose 5 mg). Examinations were performed using a commercially available ultrasound system (Sonos 5500 or 7500, Philips Medical Systems, Andover, MA). All examinations were recorded digitally. Measurements were made offline using a computer workstation (EnConcert, Philips Medical Systems, Andover, MA). All measurements were made according to our standard laboratory protocol. Two-dimensionally guided M-mode measurements were made of the right ventricular end-diastolic dimension

(RVDd), the interventricular septum in end diastole (IVSd) and end systole (IVSs), the left ventricular posterior wall in end diastole (LVPWd) and end systole (LVPWs), and the left ventricular dimension in end diastole (LVIDd) and end systole (LVIDs). M-mode measurements were made from a parasternal short-axis view at the level of the tips of the papillary muscles, with placement of the M-mode cursor guided by 2-dimensional imaging, and using the leading edge to leading edge technique. The measurements obtained by 2-dimensional echocardiography, the view from which they were obtained, and the point in the cardiac cycle are displayed in Table 1. The 2-dimensional measurements were made of the maximal dimension of the structure. Aortic and pulmonary arterial dimensions and semilunar valve diameters were measured in peak systole. Atrioventricular valve diameters were measured in diastole at the point of maximal valve excursion. Valve dimensions were measured from hinge point to hinge point. Arterial dimensions were measured from

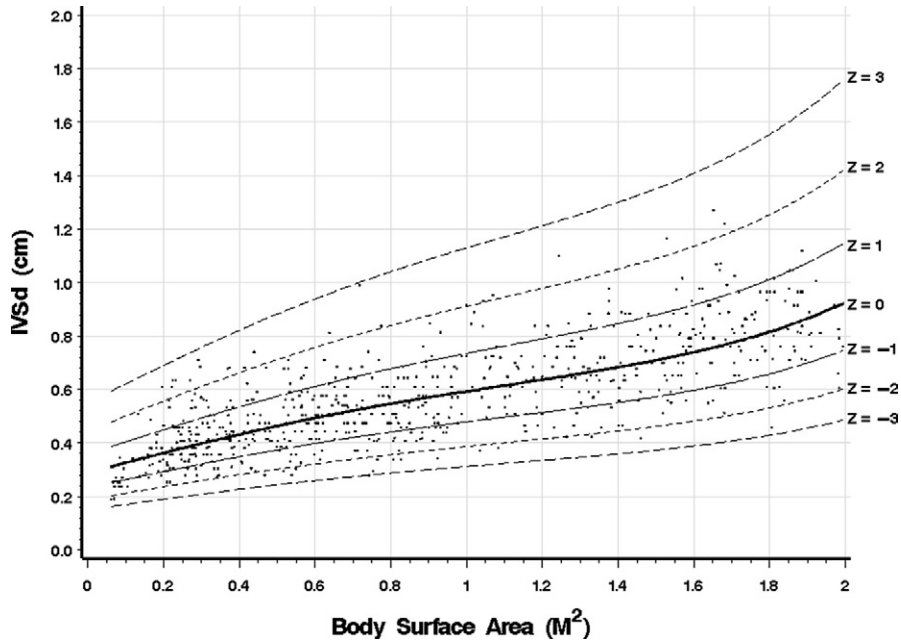


Figure 2 Scatter plot of the interventricular septal dimension in end diastole (IVSd) versus BSA.

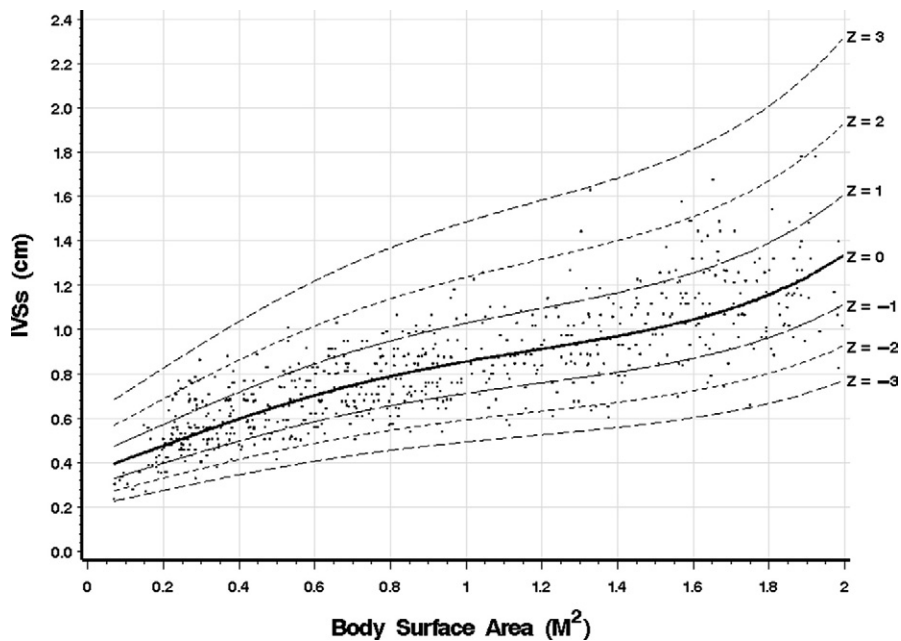


Figure 3 Scatter plot of the interventricular septal dimension in end systole (IVSs) versus BSA.

inner edge to inner edge. For any given structure, measurements were only made if excellent and unambiguous views were available. Thus, not all structures were measured in all patients. The total number of data points analyzed for each measurement ranged from 492 to 742 patients.

Statistical Methods

Body surface area (BSA) was used as the independent variable in a nonlinear regression analysis for the predicted mean value of each of the 21 echocardiographically measured structures. Because of the problem of heterogeneous variances with these measurements across the range of BSA (the larger the BSA, the larger the variance), a

logarithmic transformation using the natural logarithm was performed on all 21 structures before the fitting of the regression models for the purpose of stabilizing the variances. Several nonlinear models were considered, and a polynomial model to the third power was selected to be the final regression model. When modeling each of the 21 structures, the fourth-order polynomial term was either not statistically significant or the contribution to the overall model variations was relatively small when compared with the first-, second-, or third-order term. To keep the presentation of the study results uniform and concise, the fourth-order term was dropped. Studentized error residuals were used to detect outliers to be excluded from analysis.

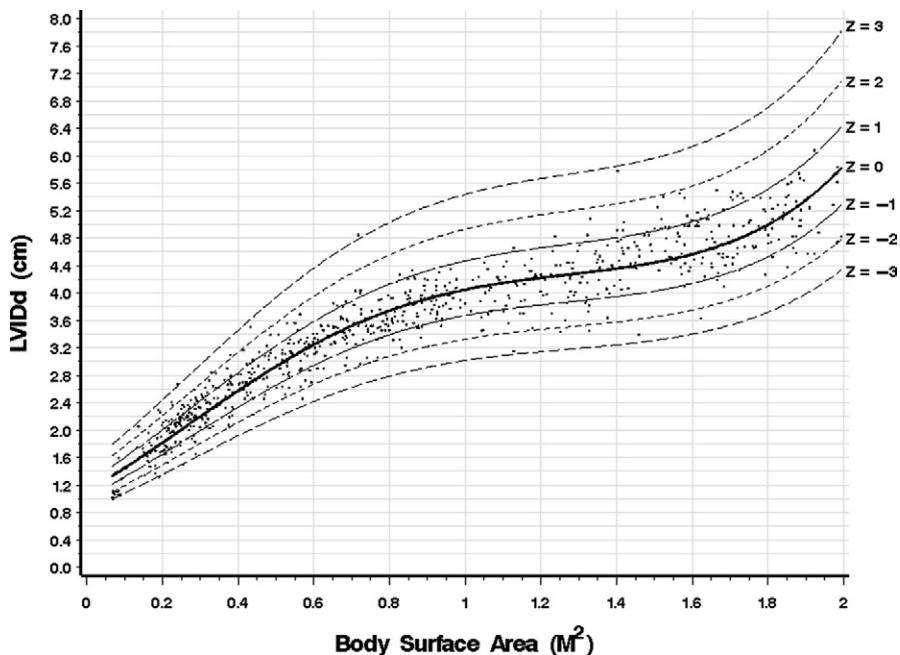


Figure 4 Scatter plot of the left ventricular internal dimension in end diastole (LVIDd) versus BSA.

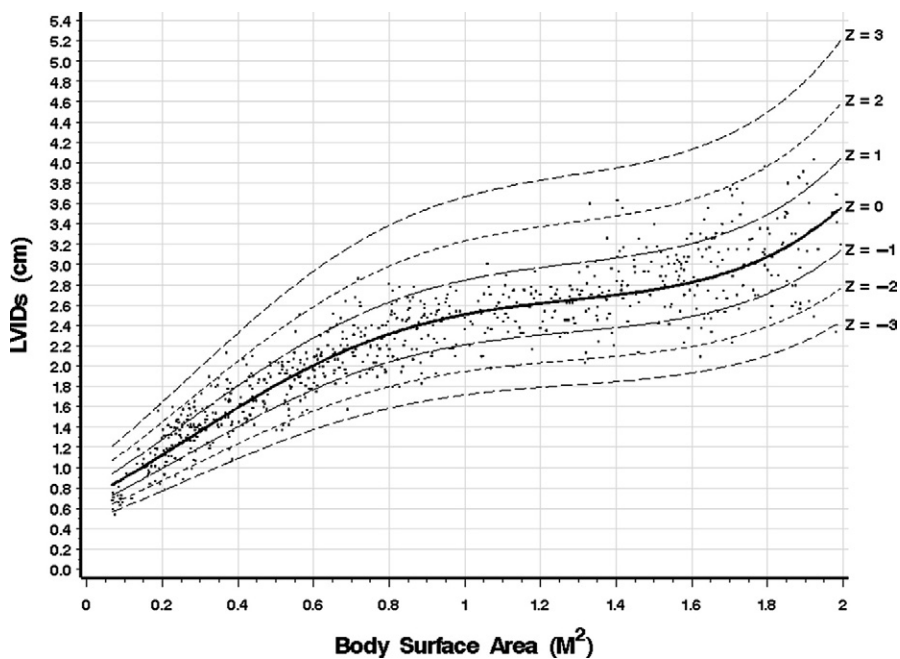


Figure 5 Scatter plot of the left ventricular internal dimension in end systole (LVIDs) versus BSA.

The first step of our analytic approach was to transform the measurement of each structure by computing its natural logarithm (ln), which is represented by y in the following.

$$y = \ln(\text{measurement}) \tag{1}$$

Next, the transformed echocardiographic measurements were entered into a nonlinear (polynomial) regression model as the dependent variable and BSA, BSA^2 , BSA^3 as the predictors (independent variables).

$$\text{Expected } y = \beta_0 + \beta_1 * BSA + \beta_2 * BSA^2 + \beta_3 * BSA^3 \tag{2}$$

Once the regression coefficients (β_0 , β_1 , β_2 , and β_3) were obtained, the equation (2) was then transformed back to the measurement's original scale by exponentiating y .

$$e^y = \exp(\hat{\beta}_0 + \hat{\beta}_1 * BSA + \hat{\beta}_2 * BSA^2 + \hat{\beta}_3 * BSA^3) \tag{3}$$

In Figures 1 to 21, the regression equations in the original unit and 6 curves corresponding to the z score = ± 1 , ± 2 , ± 3 are provided for

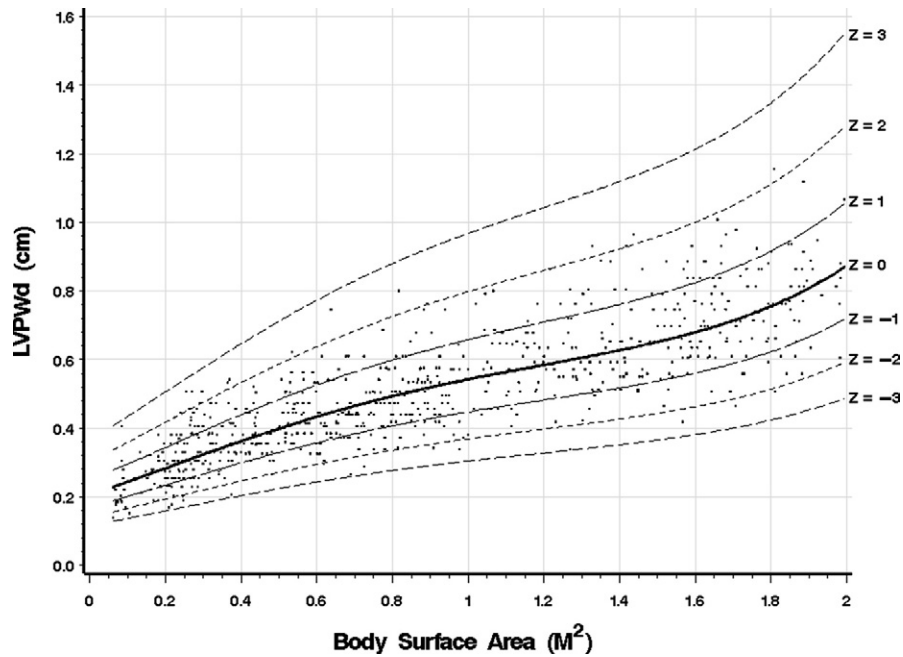


Figure 6 Scatter plot of the left ventricular posterior wall dimension in end diastole (LVPWd) versus BSA.

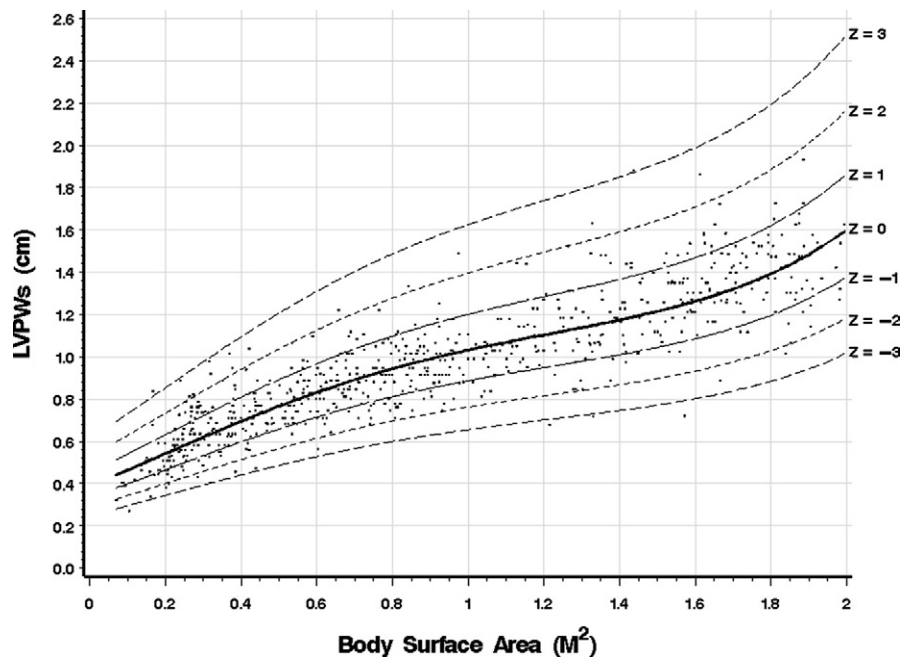


Figure 7 Scatter plot of the left ventricular posterior wall dimension in end systole (LVPWs) versus BSA.

each of the 21 echocardiographic measurements. Standardized z scores are approximately normally distributed with mean = 0 and standard deviation (SD) = 1; thus $Z = 0$ corresponds with the estimated mean, whereas $Z = \pm 1, \pm 2, \pm 3$ corresponds with $\pm 1, \pm 2, \pm 3$ SD from the estimated regression line (estimated means). In any normal distribution, 68% of the population would be classified within its mean ± 1 SD, 95.4% within mean ± 2 SD, and 99.7% within ± 3 SD. All data analyses were performed using SAS, version 9.1 (SAS Institute Inc, Cary, NC), and the least-squares method was used for the estimation of the regression curves.

RESULTS

Table 2 shows the regression results for each of the 21 echocardiographic measurements on BSA. The information presented includes the estimated regression coefficients ($\beta_0, \beta_1, \beta_2,$ and β_3) mean square error (MSE), and R^2 value (coefficient of determination). R^2 is the standard statistic used to measure how well data fit the selected regression model (goodness of fit) and has a value ranging from 0 to 1, with 1 representing a perfect fit and 0 representing a total lack of fit. Figures 1 to 21 show the scatter

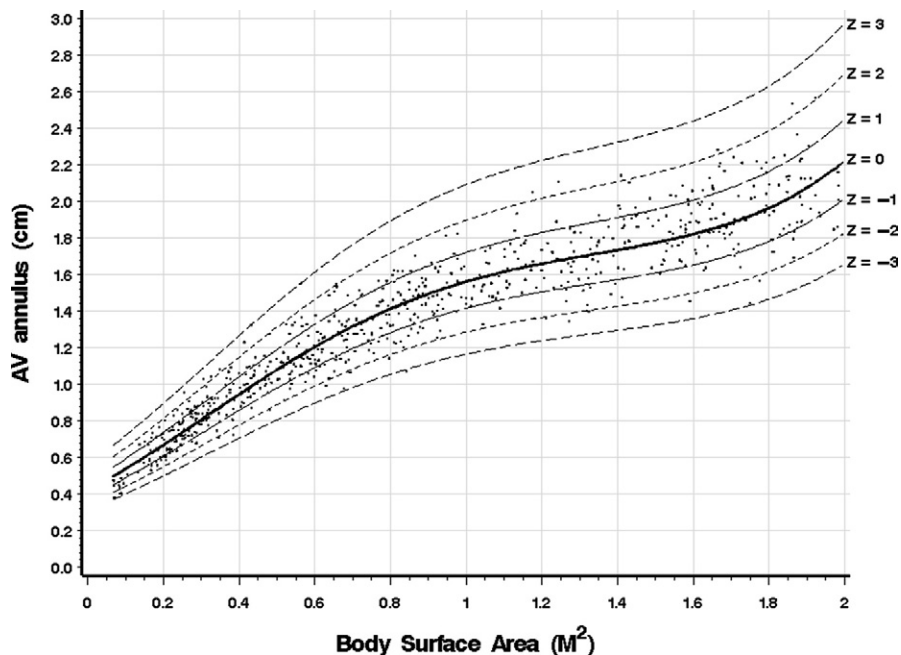


Figure 8 Scatter plot of the aortic valve annulus dimension versus BSA.

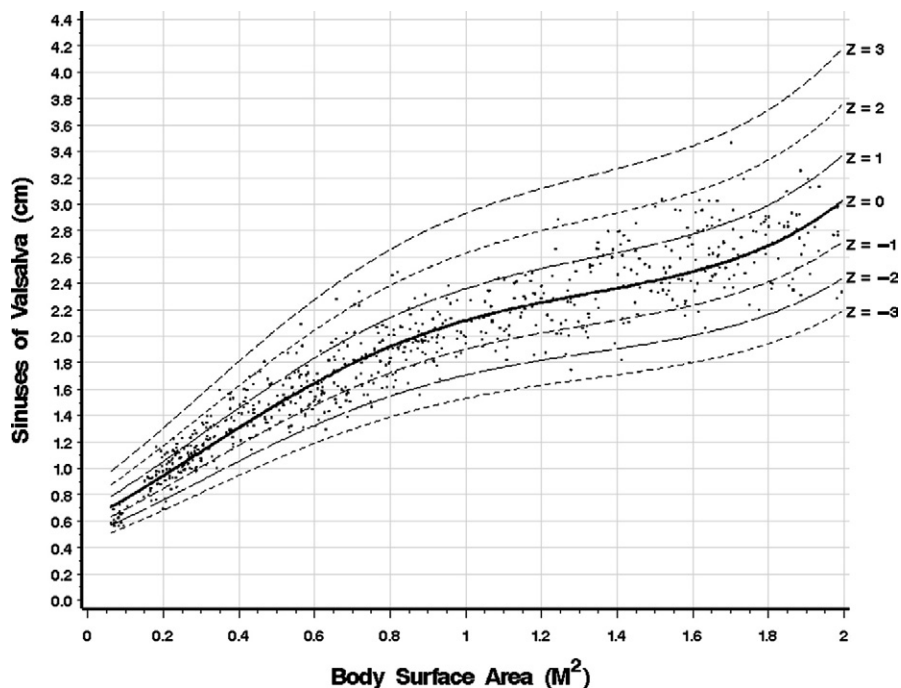


Figure 9 Scatter plot of the sinuses of Valsalva dimension versus BSA.

plots of the 21 measured structures plotted against BSA. The superimposed solid line represents the estimated regression equation (labeled as $z = 0$). The superimposed dashed lines represent the ± 1 , ± 2 , and ± 3 z values above and below the regression line. Although a constant MSE was used for each of the log-transformed echocardiographic measurements (Table 2), the lines corresponding to ± 1 , ± 2 , and ± 3 z values in Figures 1 to 21 are not parallel because the data plotted in these figures are in each measurement's original unit.

There are 2 ways one can calculate z scores for any of the 21 echocardiographic measurements using our results. One is to use the 21 graphs provided to find the approximate corresponding z score for a specific BSA, and the other is to use Table 2 values to calculate the z score directly and more precisely. As an example of how to calculate z scores by using the results in Table 2, assume a patient has a BSA of 1.4 and an IVSd of 0.4. To calculate the z score of a patient's IVSd of 0.4, the first step is to find the corresponding regression coefficients from Table 2 for IVSD, which are $\beta_0 = -1.242$,

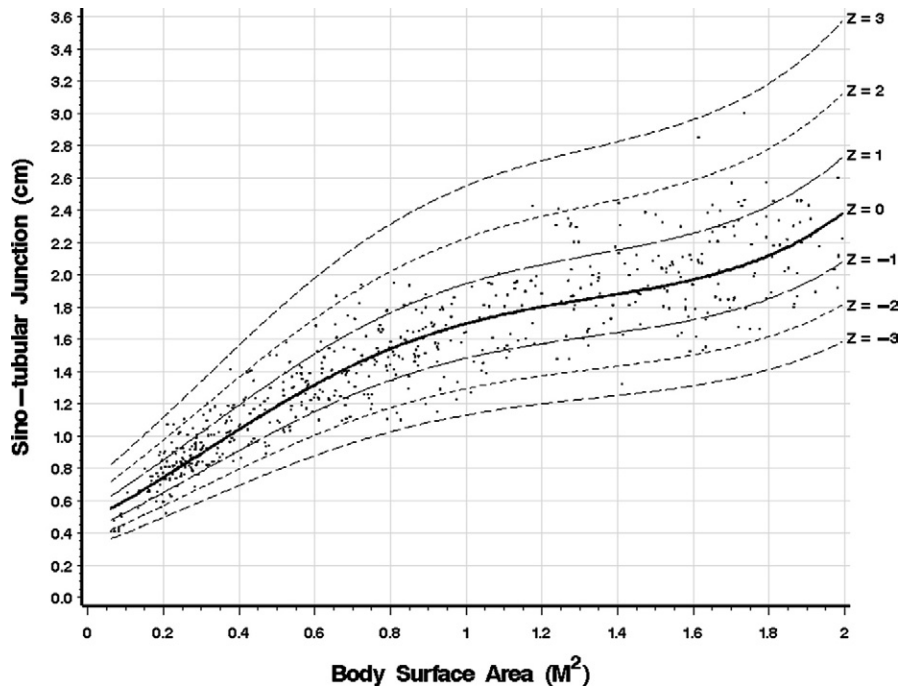


Figure 10 Scatter plot of the sino-tubular junction dimension versus BSA.

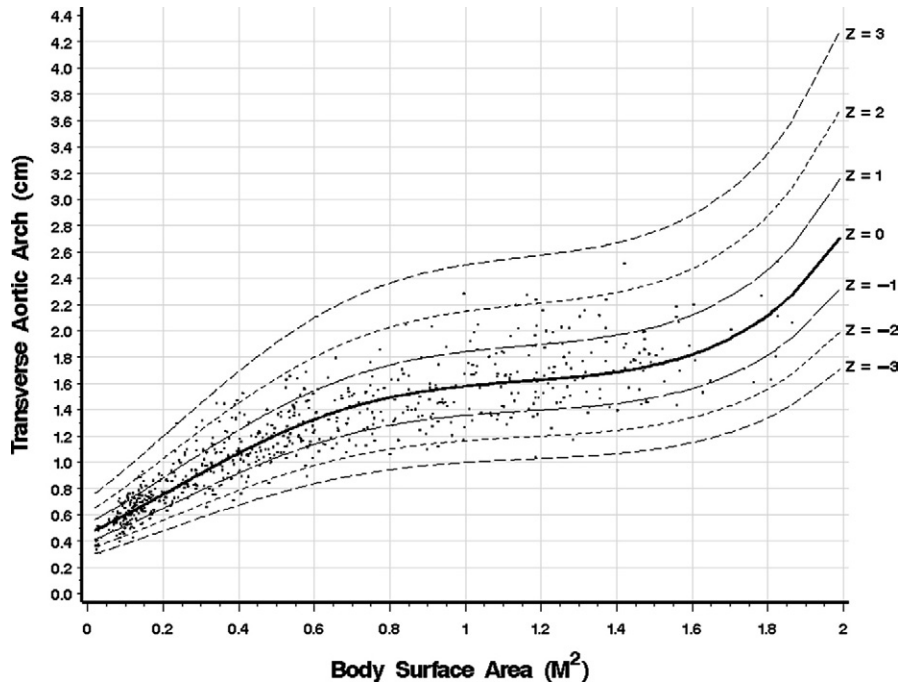


Figure 11 Scatter plot of the transverse aortic arch dimension versus BSA.

$\beta_1 = 1.272, \beta_2 = -0.762, \beta_3 = 0.208$, and $MSE = 0.046$, and insert these values into Equation (2) to obtain the mean of IVSD for $BSA = 1.4$.

$$\begin{aligned} \text{Mean } y &= -1.242 + 1.272 * 1.4 - 0.762 * 1.42^2 \\ &\quad + 0.208 * 1.43^3 \\ &= -0.384 \end{aligned}$$

Next, take the natural log of the observed IVSD (0.4) of a patient and standardize it using the following formula.

$$\begin{aligned} Z &= (\ln[\text{observed } y] - \text{Mean } y) / \sqrt{MSE} \\ &= (\ln[0.4] - [-0.384]) / \sqrt{0.046} \\ &= -2.48 \end{aligned}$$

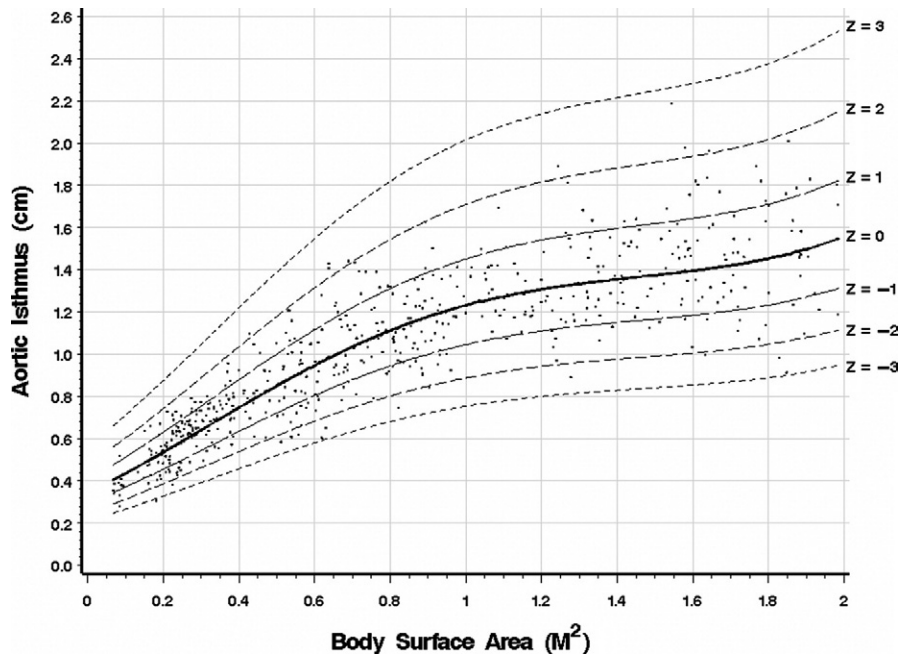


Figure 12 Scatter plot of the aortic isthmus dimension versus BSA.

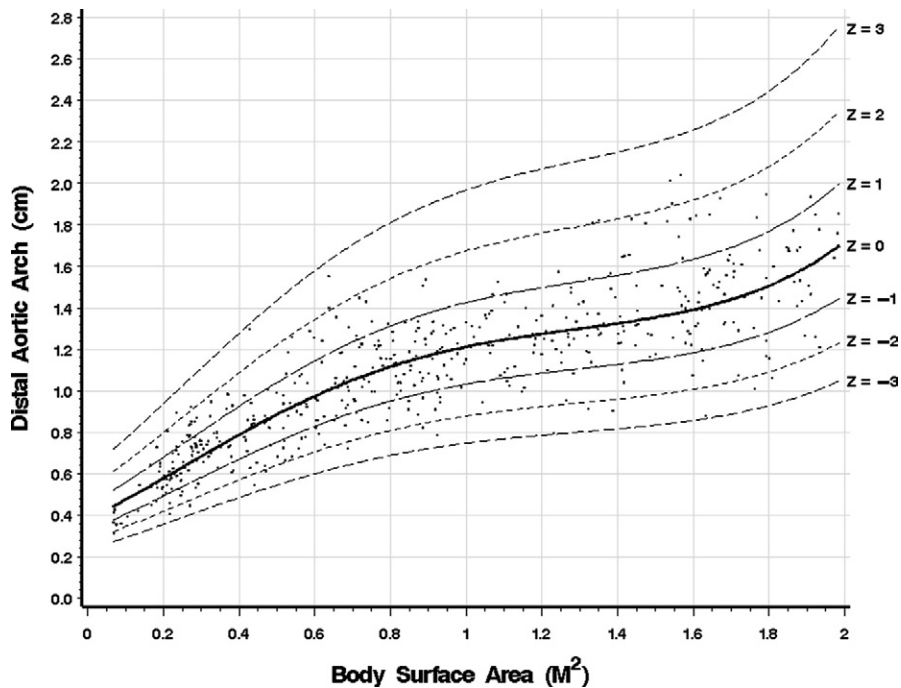


Figure 13 Scatter plot of the distal aortic arch dimension versus BSA.

DISCUSSION

The detailed measurement of cardiac structures remains a crucial aspect in the management of children with various types of congenital and acquired cardiac disease. Decisions on the type and timing of interventions often rely to a large extent on these measurements. For example, the relative hypoplasia of a chamber or valve may dictate the choice of a 4-chamber repair versus a single-ventricle palliation. Similarly, chamber dilation from a congenital shunt lesion may be compared with these normal values to

determine the need for surgical intervention. Because these structures grow with the child throughout childhood, interpretation of these measurements must take into account a patient's body size.

Despite the importance of these measurements in clinical practice, a comprehensive set of normative data derived from a large cohort of patients are lacking. Many larger pediatric echocardiography laboratories have developed their own reference normal data to use in their echocardiography reporting and as part of their clinical decision making. Smaller laboratories without ac-

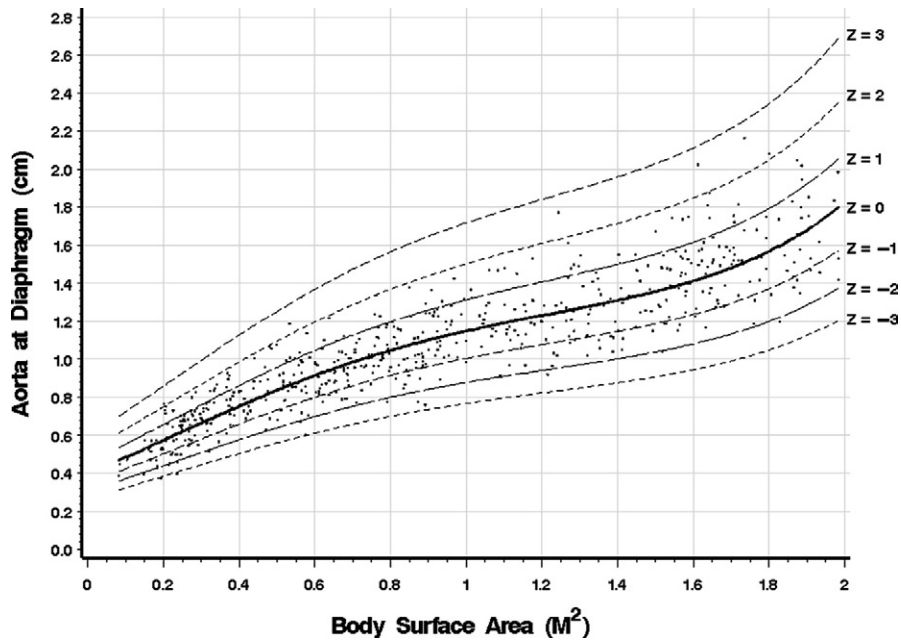


Figure 14 Scatter plot of the aortic dimension at the level of the diaphragm versus BSA.

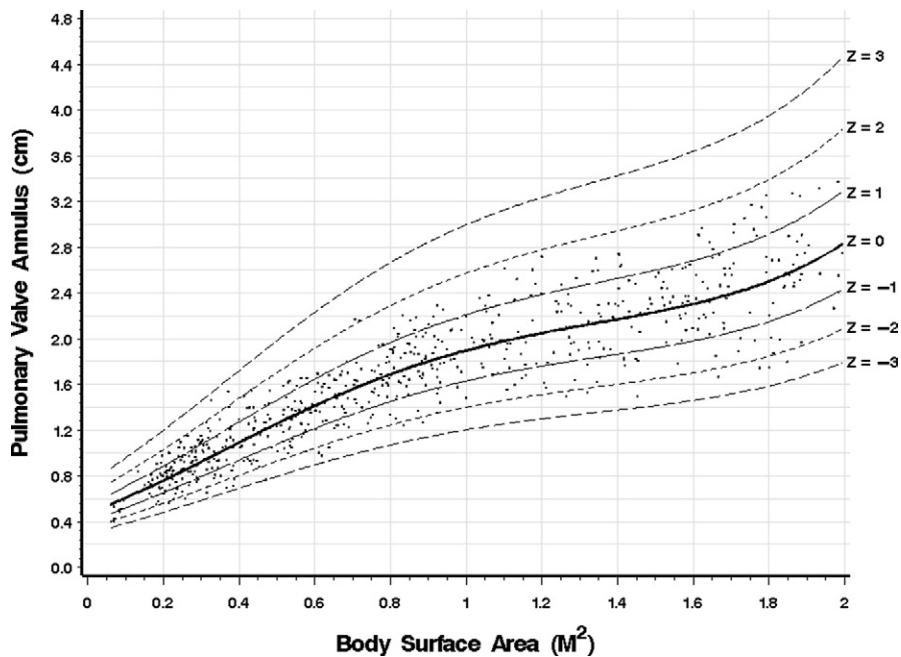


Figure 15 Scatter plot of pulmonary valve annulus dimension versus BSA.

cess to this data are reliant on previously published normative data.

Previous publications currently in clinical use have significant limitations. Some commonly used z-score nomograms are based on formalin-fixed pathologic specimens.^{1,2} These measurements tend to significantly underestimate the dimensions of the cardiac structures in vivo and are inappropriate for use with clinical echocardiography. Many older studies were performed using exclusively unguided M-mode measurements.³⁻⁶ Although this technique is well standardized and validated in the measurement of left ventricular internal dimension and wall thickness, it is not appropriate for measurement

of valve annuli and other cardiac structures where direct visualization of the structure by 2-dimensional echocardiography is important. Other published normative data are limited by relatively small numbers of pediatric patients and limited number of measured cardiac structures.⁷⁻¹⁵

Kampmann et al¹⁵ reported normal M-modes values in more than 2000 healthy European children. However, this report focused solely on M-mode measurements. Measurements of valve annuli and detailed measurements of the aortic arch and pulmonary arteries are lacking. In this publication, the r^2 values reported along with the estimated regression models look impressive at first glance, because

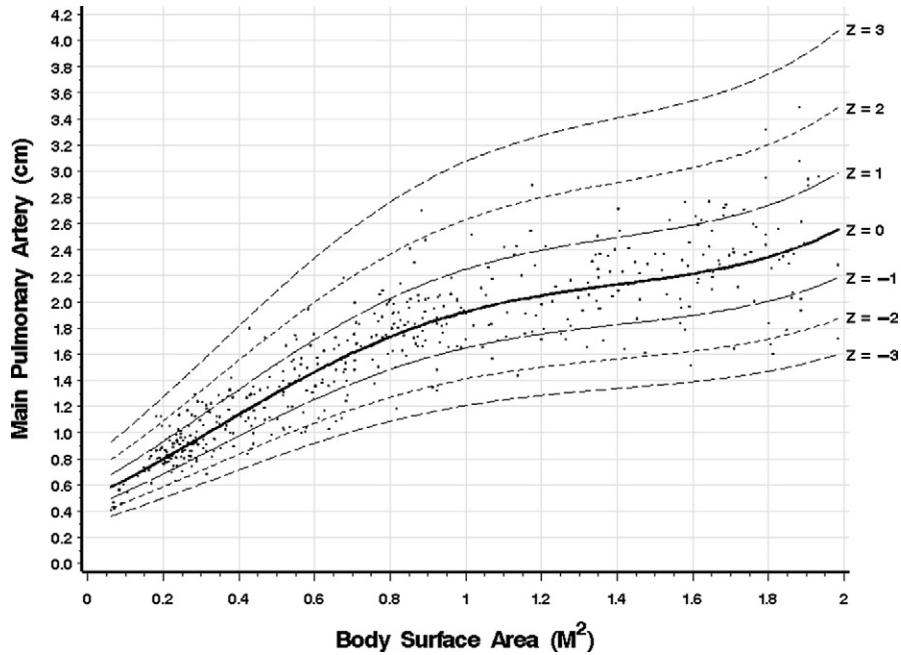


Figure 16 Scatter plot of the main pulmonary artery dimension versus BSA.

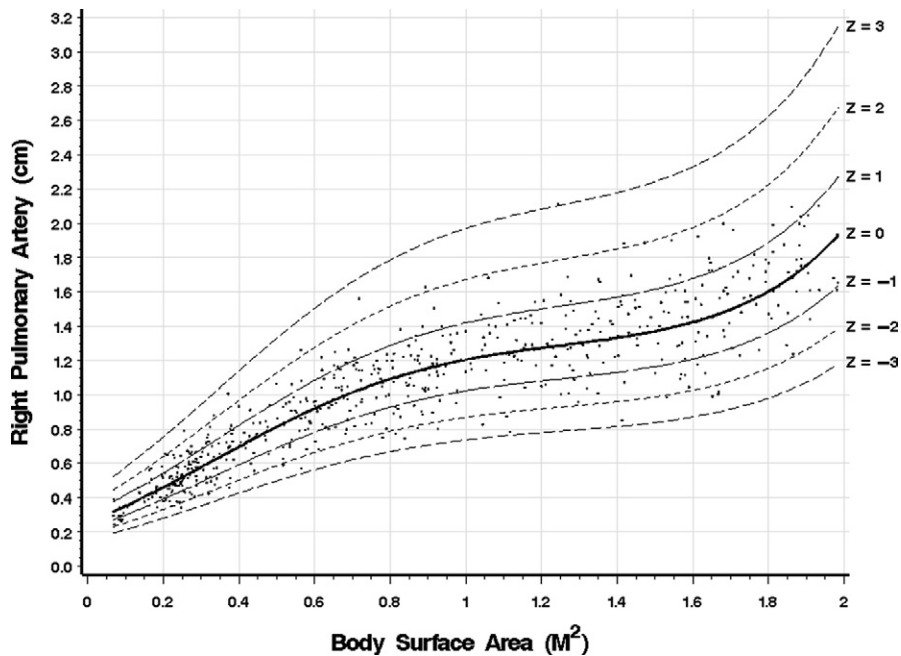


Figure 17 Scatter plot of the right pulmonary artery dimension versus BSA.

these values are all in the range of 0.97 to 0.99. However, on close examination, these r^2 are not the commonly used R^2 (coefficient of determination), which measures the goodness-of-fit of a regression model. Instead, these r^2 values are the square of the correlation between the estimated regression curves and the 50th percentiles of arbitrarily grouped data based on BSA values and thus do not reflect how well the regression models perform. We compared one of the models they used in 9 of the 11 measures: $\ln(\text{measurement}) = \ln(\alpha) + \beta * \ln(\text{BSA})$ with our model: $\ln(\text{measurement}) = \beta_0 + \beta_1 * \text{BSA} + \beta_2 * \text{BSA}^2 + \beta_3 * \text{BSA}^3$. The performance of the 2 mathematic models did not differ significantly, based on the R^2 statistic. In

addition, the 7 non-smooth percentile curves provided for each of the measures were not derived directly from the results of the regression analysis but instead were based on the original data points. This approach lacks statistical rationale because it did not make use of the error variance estimates resulting from the regression modeling.

Daubeney et al¹³ published the largest series to date of 2-dimensionally derived echocardiographic data. This article used the same mathematic model as Kampmann et al¹⁵ but derived their confidence bands (± 1 SD and ± 2 SD) in a manner similar to our approach. However, this series included only 125 patients and 15 different cardiac measurements.

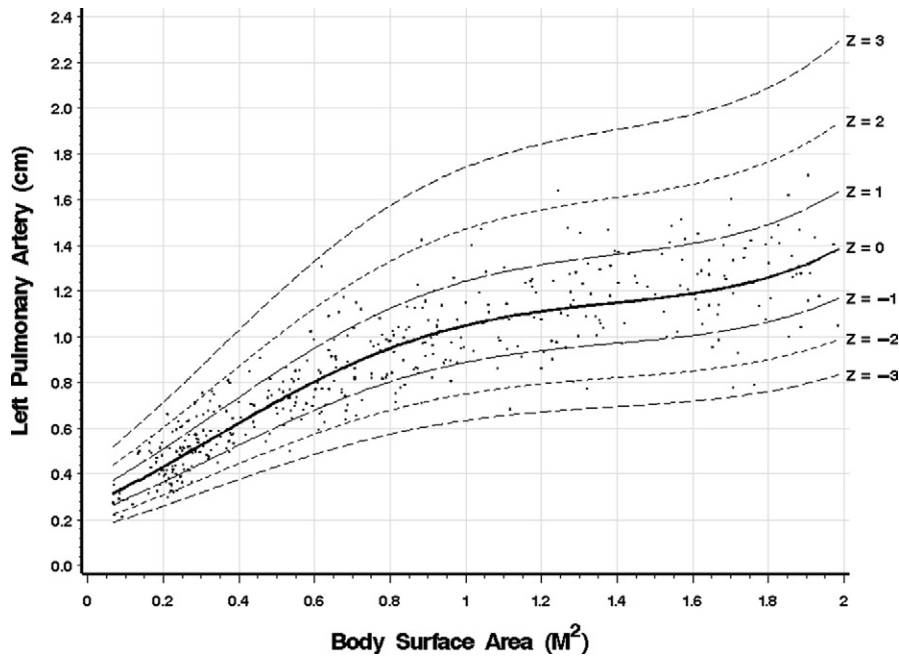


Figure 18 Scatter plot of the left pulmonary artery dimension versus BSA.

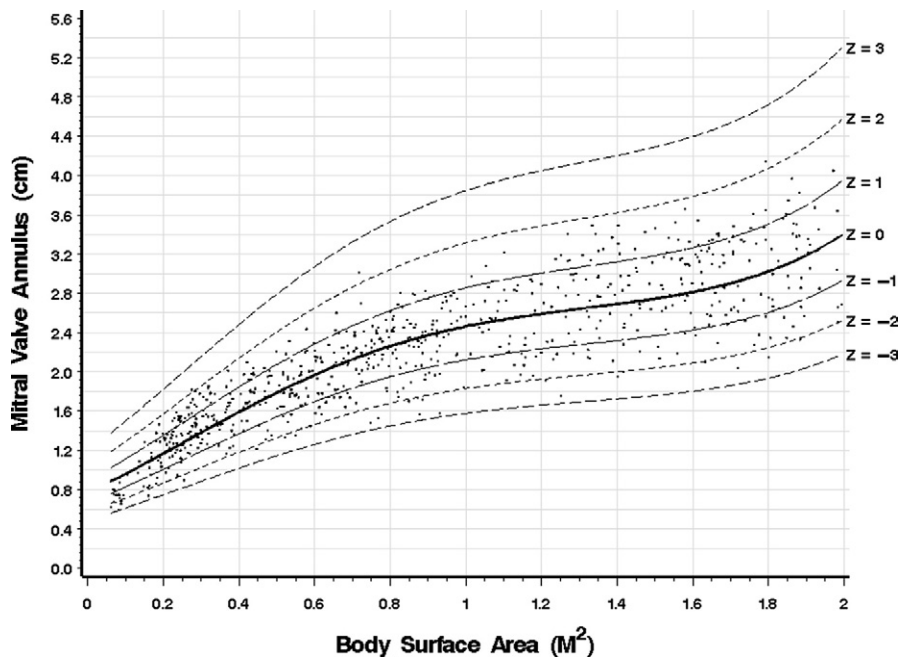


Figure 19 Scatter plot of the mitral valve annulus dimension versus BSA.

The current report includes measurements of 21 commonly measured cardiac structures in more than 700 patients over a wide range of ages and body sizes. Although this does not represent a truly unselected population, every effort was made to exclude any patient with known or possibly subclinical cardiac disease. This report also includes 82 patients with a BSA ≤ 0.25 m², a subgroup not well represented in any previously published datasets. Tacy et al⁹ had previously reported valve annulus dimensions in 103 neonates ages 0 to 10 days. No other cardiac structures were examined in that report. In addition, the variance of the measurements was not normalized

across the range of body size; thus, accurate z scores could not be calculated.

Previously published studies have related the size of cardiac structures to height^{7,9,10,16} BSA,^{6,8,11-14} or weight.^{9,16} Roge et al⁴ demonstrated that height, weight, and BSA, as well as the cube root of weight, were all so strongly correlated that regressions using any 1 of those 4 variables were equivalent for all practical purposes. Hemodynamic data were generally expressed in relation to BSA.¹⁷ In addition, all modern echocardiographic equipment is programmed to calculate BSA. Thus, the most widespread clinical

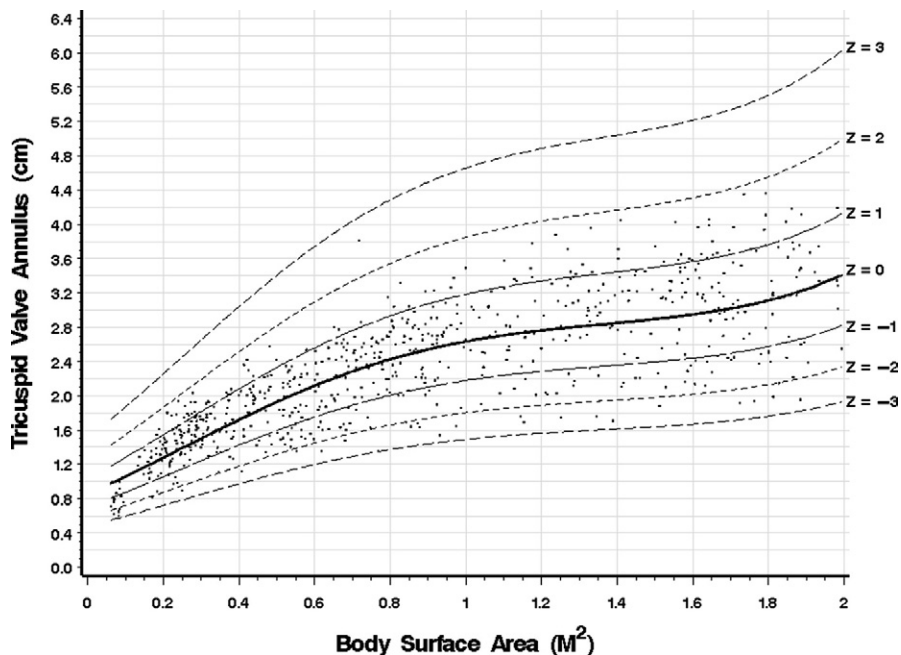


Figure 20 Scatter plot of the tricuspid valve annulus dimension versus BSA.

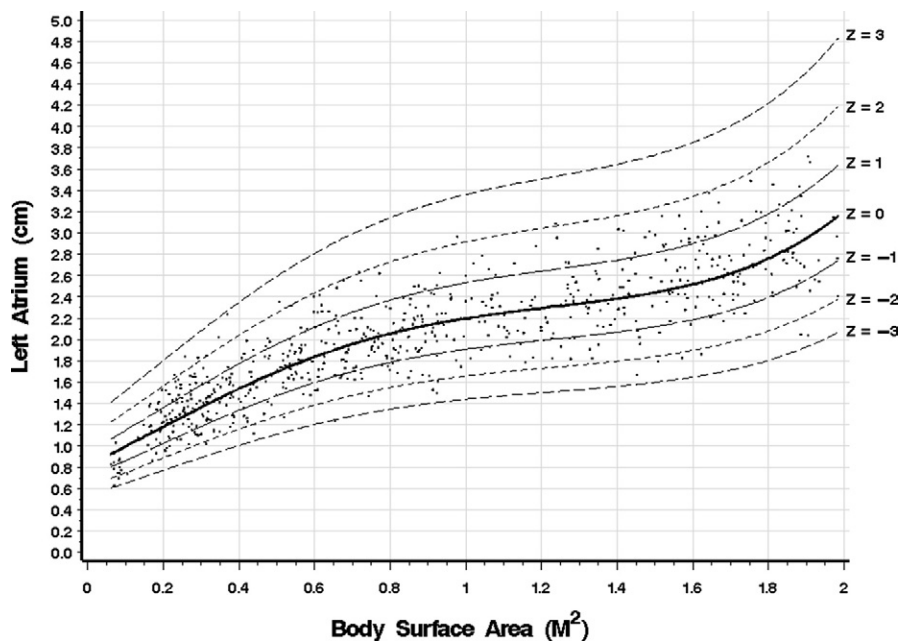


Figure 21 Scatter plot of the left atrium dimension versus BSA.

practice has become to relate the size of cardiac structure to BSA in children.

This report makes exclusive use of digital echocardiographic equipment to derive normative pediatric data. In most of the previously published studies, echocardiograms were recorded in analog format on videotape. The use of a digital format has several advantages and lessens the possibility of systematic error that can be introduced when using analog storage. Image quality is higher because the images appear exactly as they were originally recorded from the machine without any degradation from the videotaping process. Quantification is easier, because spatial and temporal calibra-

tion are built directly into the image, eliminating the need for offline recalibration. Finally, accuracy and reproducibility are improved over analog techniques.¹⁸

CONCLUSIONS

We report the dimensions of 21 commonly measured cardiac structures in a large cross-sectional cohort of normal infants, children, and adolescents, relative to BSA. Regression equations are presented for the mean dimensions and variances across the range of body size. These equations may be used in the calculation of z scores that are

Table 2 Coefficients for regression equations relating echocardiographic measurements and body surface area, and the mean square error and coefficient of determination

Measurement	Intercept (β_0)	BSA (β_1)	BSA ² (β_2)	BSA ³ (β_3)	MSE	R ²
RVDd	-0.317	1.850	-1.274	0.335	0.058	0.604
IVSd	-1.242	1.272	-0.762	0.208	0.046	0.606
IVSs	-1.048	1.751	-1.177	0.318	0.034	0.695
LVIDd	0.105	2.859	-2.119	0.552	0.010	0.922
LVIDs	-0.371	2.833	-2.081	0.538	0.016	0.875
LVPWd	-1.586	1.849	-1.188	0.313	0.037	0.739
LVPWs	-0.947	1.907	-1.259	0.330	0.023	0.794
Aortic valve annulus	-0.874	2.708	-1.841	0.452	0.010	0.934
Sinuses of Valsalva	-0.500	2.537	-1.707	0.420	0.012	0.916
Sinotubular junction	-0.759	2.643	-1.797	0.442	0.018	0.878
Transverse aortic arch	-0.790	3.020	-2.484	0.712	0.023	0.865
Aortic isthmus	-1.072	2.539	-1.627	0.368	0.027	0.825
Distal aortic arch	-0.976	2.469	-1.746	0.445	0.026	0.792
Aorta at diaphragm	-0.922	2.100	-1.411	0.371	0.018	0.842
Pulmonary valve annulus	-0.761	2.774	-1.808	0.436	0.023	0.873
Main pulmonary artery	-0.707	2.746	-1.807	0.424	0.024	0.857
Right pulmonary artery	-1.360	3.394	-2.508	0.660	0.027	0.873
Left pulmonary artery	-1.348	2.884	-1.954	0.466	0.028	0.842
Mitral valve annulus	-0.271	2.446	-1.700	0.425	0.022	0.826
Tricuspid valve annulus	-0.164	2.341	-1.596	0.387	0.036	0.726
Left atrium	-0.208	2.164	-1.597	0.429	0.020	0.801

BSA, Body surface area; MSE, mean square error; RVDd, right ventricular end-diastolic dimension; IVSd, Interventricular septum in end diastole; IVSs, interventricular septum in end systole; LVIDd, left ventricular dimension in end diastole; LVIDs, left ventricular dimension in end systole; LVPWd, left ventricular posterior wall in end diastole; LVPWs, left ventricular posterior wall in end systole.

commonly used in clinical decision making for pediatric patients with congenital or acquired cardiac disease.

REFERENCES

- Kirklin JW, Barratt-Boyes BG, editors. Cardiac surgery. 2nd ed. Edinburgh: Churchill Livingstone; 1993:30-55.
- Rowlatt UF, Rimoldi HJA, Lev M. The quantitative anatomy of the normal child's heart. *Pediatr Clin North Am* 1963;10:499-588.
- Henry WL, Ware J, Gardin JM, et al. Echocardiographic measurements in normal subjects. Growth-related changes that occur between infancy and early adulthood. *Circulation* 1978;57:278-85.
- Roge CL, Silverman NH, Hart PA, et al. Cardiac structure growth pattern determined by echocardiography. *Circulation* 1978;57:285-90.
- Henry WL, Gardin JM, Ware JH. Echocardiographic measurements in normal subjects from infancy to old age. *Circulation* 1980;62:1054-61.
- Epstein ML, Goldberg SJ, Allen HD, et al. Great vessel, cardiac chamber, and wall growth patterns in normal children. *Circulation* 1975;51:1124-9.
- Sheil ML, Jenkins O, Sholler GF. Echocardiographic assessment of aortic root dimensions in normal children based on measurement of a new ratio of aortic size independent of growth. *Am J Cardiol* 1995;75:711-15.
- King DH, Smith EO, Huhta JC, et al. Mitral and tricuspid valve annular diameter in normal children determined by two-dimensional echocardiography. *Am J Cardiol* 1985;55:787-9.
- Tacy TA, Vermilion RP, Ludomirsky A. Range of normal valve annulus size in neonates. *Am J Cardiol* 1995;75:541-3.
- Nidorf SM, Picard MH, Triulzi MO, et al. New perspectives in the assessment of cardiac chamber dimensions during development and adulthood. *J Am Coll Cardiol* 1992;19:983-8.
- Snider AR, Enderlein MA, Teitel DF, et al. Two-dimensional echocardiographic determination of aortic and pulmonary artery sizes from infancy to adulthood in normal subjects. *Am J Cardiol* 1984;53:218-24.
- Roman MJ, Devereux RB, Kramer-Fox R, et al. Two-dimensional echocardiographic aortic root dimensions in normal children and adults. *Am J Cardiol* 1989;64:507-12.
- Daubeney PE, Blackstone EH, Weintraub RG, et al. Relationship of the dimension of cardiac structures to body size: an echocardiographic study in normal infants and children. *Cardiol Young* 1999;9:402-10.
- Zilberman MV, Khoury PR, Kimball RT. Two-dimensional echocardiographic valve measurements in healthy children: gender-specific differences. *Pediatr Cardiol* 2005;26:356-60.
- Kampmann C, Wiethoff CM, Wenzel A, et al. Normal values of M mode echocardiographic measurements of more than 2000 healthy infants and children in central Europe. *Heart* 2000;83:667-72.
- Rimoldi HJA, Lev M. A note on the concept of normality and abnormality n quantification of pathologic findings in congenital heart disease. *Pediatr Clin North Am* 1963;10:589-91.
- Gutgesell HP, Rembold CM. Growth of the human heart relative to body surface area. *Am J Cardiol* 1990;65:662-8.
- Thomas JD, Adams DB, Devries S, et al. Guidelines and recommendations for digital echocardiography. *J Am Soc Echocardiogr* 2005;18:287-97.